THE ASTRONOMICAL JOURNAL

VOLUME 79 May 1974 ~ No. 1420 *NUMBER 5*

Ooty occultations of 76 radio sources

Vijay K. Kapahi, Mohan N. Joshi, and N. V. G. Sarma

Radio Astronomy Group, Tata Institute of Fundamental Research, Homi Bhabha Road, Bombay-400005, India

(Received 17 January 1974)

Positional and structural information derived from lunar occultations observed at 327 MHz is presented for 76 radio sources, most of them of flux density less than $2\times10^{-26}\mathrm{Wm^{-2}Hz^{-1}}$. Only 16 sources are optically identified. Two of the stronger sources in the list, viz. PKS 1417-19 and MSH 16-205 have a head–tail type of radio structure. PKS 1417-19 appears to be associated with a small chain of faint galaxies. It is interesting that a close group of five radio sources, each with flux density $\geq$0.5 f.u. appears to be physically associated with the cluster Zw 0210.1+1857. One of the five sources coincides with a 19-mag BSO, while none of the other four is identified with an optical object on the basis of positional agreement.

THE observations of lunar occultations made at 327 MHz with the Ooty radio telescope have led to the determination of accurate source positions and brightness distributions for a large number of weak radio sources. The positions and structures obtained from the occultations are being used also to make reliable optical identifications from the prints of the Palomar Sky Survey. The results for a total of 110 radio sources have been reported earlier (Swarup *et al.* 1971; Kapahi 1971; Kapahi *et al.* 1972, 1973a, 1973b, and Joshi *et al.* 1973). In this paper, we present the results for another 76 sources, a majority of them previously uncataloged and in the flux-density range of 0.3 f.u.–2 f.u. (1 f.u.$=10^{-26}$ Wm^{-2} Hz^{-1}). The sources were occulted during 1970 and 1971 and at least two occultations were observed for each source. Positive identifications have been found for only 16 sources; ten with galaxies, five with blue stellar objects (BSO's), and one with a stellar object. Identifications for four sources made earlier by other observers, have not been confirmed by the more accurate observations reported here. An analysis of the radio structures determined from lunar occultations will be presented later.

RESULTS

The methods of observation and analysis of occultations and the procedure for the estimation of accurate optical positions of identified objects or of objects closest to the radio positions have been described in the earlier papers. Reference should be made in particular to Kapahi *et al.* (1973b), where a detailed explanation is given to the format of the tabular presentation of the results and to the error estimates of the different entries.

In Table I we give the structural information and in Table II the radio and optical positions for the 76 radio sources. Finding charts for the 13 new identifications are presented in Plate I, (p. 659).

A. Additional Comments on Individual Sources

0134+142. There is a possible component of lower surface brightness extending up to ~30 arcsec west or southwest with $\leq$25% of the total flux.

0210+188 and 0210+190. Both sources lie close to the center of the cluster Zw 0210.1+1857 and are likely to be associated with it. Zwicky *et al.* (1965) have classified the cluster as 'medium compact' and 'medium distant,' with a population of 120 in a 'diameter' of ~1°.2. Neither of the two sources coincides with a galaxy in the cluster. There are three galaxies of 15–16 mag at about 1′.5 E and 1′.1 N; 2′.0 E and 2′.3 N, and 2′.8 E and 0′.9 N of 0210+190.

In an earlier list (Kapahi *et al.* 1973b), we have reported the occulations of three other sources viz. OTL 0208+183, 0209+184, and 0209+181, which are near the boundary (as marked by Zwicky *et al.*) of the same cluster. The five radio sources, all with a flux density $\geq$0.5 f.u. lie within a circle of radius ~30 arcmin on the sky. From the known number density, less than one source of this intensity is expected in such a circle chosen at random. Thus, there is a strong suggestion that the five sources are physically associated with the cluster. It is, therefore, interesting to note that while none of the five sources is identified with a galaxy, one, viz. 0208+183, coincides in position with a 19-mag BSO (finding chart given in Kapahi *et al.* 1973b) which lies only ~10 arcsec away from a 17.5-mag galaxy. In view of the importance of establishing the discrepant

Table I. Structure of 76 radio sources at 327 MHz.

(1)	(2)	(3)	(4)	(5)	(6)	(7)		(8)	(9)	(10)	(11)
				Observed data				Derived structure			
Source OTL	Other catalog No.	Flux 327 MHz	No. of occult-ations	β_e	PA of occln.	Component sizes A	B	PA A to B	Comp. Sepn.	Flux ratio A/B	Remarks
0023+058	···	0.6 f.u.	2	4.1″ 4.1	109° 163	<3″ <4	···	···	···	···	···
0134+142	4C 14.07	1.2	4	8 8	95 225	~12 ~13	···	···	···	···	(N)
0141+157	···	0.4	4	8 8	67 225	~8 ≤7	···	···	···	···	···
0210+188	···	0.5	2	8 8	59 246	≤6 ≤6	···	···	···	···	···
0210+190	H 0210+18	0.8	2	4.1 2.2	28 281	≤3 ~3.5	···	···	···	···	···
0246+219	···	1.0	2	2.1 2.1	3 335	~4 ~2.5	~(6) ~4	25°	9″	1.2	(N)
0246+217	···	0.4	2	4.2 5.1	72 265	~5 ~(9)	···	···	···	···	···
0346+253	···	0.5	2	8 8	82 266	≤6 ≤7	···	···	···	···	···
0505+278	B2 0505+27	1.1	3	5 10	30 265	~10 ~16	···	···	···	···	(N)
0513+279	B2 0513+27	0.8	4	3.2 3.2	75 301	~4 ≤2.5	···	···	···	···	···
0532+281	B2 0532+28	1.1	2	4 4	24 311	≤12 ~7	≤12 ≤5	90	17	1.4	(N)
0547+279	B2 0547+27	0.5	2	15 15	85 286	≤12 ≤12	···	···	···	···	···
0608+275	B2 0608+27	0.4	2	4.1 4.1	145 214	~7 ~4	···	···	···	···	···
0609+276	B2 0609+27B	0.8	4	2.1 2.1	117 248	~5 <2	<2 <2	158	12	0.7	···
0618+272	B2 0618+27	0.6	4	10 10	80 88	~22 ~24	···	···	···	···	···
0619+270	···	0.5	2	8 8	54 300	~10 <8	···	···	···	···	···
0620+270	···	0.4	2	10 8	40 315	≤10 ≤6	≤12 ≤6	8	28	2	···
0638+273	OH 264	1.0	2	2.2 1.4	85 304	≤2 ≤1.4	···	···	···	···	···
0706+261	4C 26.26	2.5	4	1.3 1.3	86 283	~1.5 ≤2	~1.5 ≤1.2	140	3.5	0.7	(N)
0719+255	PKS 0719+25	0.9	2	8 8	81 290	~23 ~54	···	···	···	···	Cx, (N)
0725+244	PKS 0725+24	1.6	2	2.2 2.2	127 289	<1.5 <1.5	···	···	···	···	···
0725+248	B2 0725+24B	0.7	2	4 10	159 258	~5 <10	···	···	···	···	···
0817+212	···	0.3	2	2.2 4	109 321	<2 <3	~4 ~5	118	11	1.5	···
0818+214	OJ 230	0.6	2	8 8	7 64	~12 ~12	···	···	···	···	···
0818+217	···	0.7	2	4 4	114 316	~15 ~16	≤4 ≤3	84	22	0.9	···

TABLE I (*continued*)

(1) Source OTL	(2) Other catalog No.	(3) Flux 327 MHz	(4) No. of occultations	(5) β_e	(6) Observed data: PA of occln.	(7) Observed data: Component sizes A	Component sizes B	(8) Derived structure: PA A to B	(9) Comp. Sepn.	(10) Flux ratio A/B	(11) Remarks
0823+207	...	0.7	2	2.3 2.3	137 284	∼3 ∼3	...	...	...	...	...
0854+191	...	0.25	2	4 4	68 347	≤3 ≤3	...	...	...	...	...
0856+178	...	0.5	2	8 8	155 272	≤6 ≤6	...	...	...	...	...
0904+174	...	0.4	2	8 15	96 285	≤7 <15	...	...	...	...	(N)
0907+185	PKS 0907+18	2.0	2	4 1.3	99 333	∼5.5 ∼2.5	...	...	...	...	(N)
0909+165	4C 16.27	5.4	2	1.3 8	142 294	∼1.3 <8	≤1.3 <8	(24)	(13)	1.6	(N)
0937+144	...	0.8	2	2.2 2.1	116 318	≤1.6 ≤1.8	...	...	...	...	...
0952+128	...	0.4	2	10 10	129 305	<10 <10	...	...	...	...	(N)
0954+126	...	0.4	2	8 4	100 346	≤10 ≤3.5	...	...	...	...	...
0954+125	...	0.5	2	4 4	105 343	<4 ≤4	...	...	...	...	(N)
1022+093	...	0.9	2	4 8	115 322	∼9 ∼13	...	...	...	...	...
1037+067 }	4C 06.41	2.0	4	4 1.2	85 159	<3 <1	...	...	...	...	(N)
1038+064 }	4C 06.41	1.7	2	4 4	109 331	<4 <4	...	...	...	...	(N)
1105+037	PKS±4°	1.2	2	2.2 3.1	138 304	∼3.5 ∼3.5	...	...	...	...	...
1123+012	PKS±4°	1.2	2	2.2 1.3	12 85	∼3.5 ∼2	...	...	...	...	PD, (N)
1155−029	PKS±4°	0.9	3	4 8	156 305	≤3 ≤6	...	...	...	...	...
1239−086	PKS 1239−08	1.7	2	1.4 1.4	128 324	≤1.2 <1.2	...	...	...	...	...
1241−089	...	0.3	2	4 8	90 351	∼6 <8	...	...	...	...	...
1253−109	...	0.5	4	5 5	109 264	≤5 ∼5	...	...	...	...	...
1316−128	...	0.8	2	4 4	126 313	∼4 ∼4	...	...	...	...	...
1417−192	PKS 1417−19	5.5	5	2.1 2.1	66 358	∼4 ∼7	...	30	...	...	Cx, (N)
1431−202	...	0.5	2	10 10	108 282	<8 <8	...	...	...	...	...
1547−254	...	0.9	2	3.2 3.2	137 276	∼5 ≤2.5	...	...	...	...	...
1628−268	MSH 16−205	8.0	4	2.1 2.1	43 356	∼6 ∼3	...	103	...	...	Cx, (N)

TABLE I (*continued*)

(1) Source OTL	(2) Other catalog No.	(3) Flux 327 MHz	(4) No. of occult-ations	(5) β_e	(6) Observed data: PA of occln.	(7) Observed data: Component sizes A	(7) Observed data: Component sizes B	(8) Derived structure: PA A to B	(9) Derived structure: Comp. Sepn.	(10) Derived structure: Flux ratio A/B	(11) Remarks
1650−283	...	0.5	2	8	111	∼11	...	...	...	...	...
				8	256	≤6					
1653−281	...	0.6	5	5	148	∼6	...	...	...	...	...
				5	69	∼12					
1657−281	...	0.5	5	15	95	∼30	...	...	...	...	(N)
				30	295	∼35					
1709−281	MSH 17−204	13	6	1.2	72	≤1.2	≤1.2	146	15	1.3	(N)
				1.2	328	∼1.8	∼1.9				
1711−285	...	1.1	2	2.1	146	∼2	...	...	...	...	...
				2.1	228	≤1.6					
1800−278	MSH 17−217	12.0	2	2.2	109	∼9	∼9	159	43	1.8	(N)
				2.2	222	∼15	≤10				
1818−269	...	1.5	2	15	25	∼60	...	...	...	...	Cx
				15	297	∼35					
1827−279	...	0.7	2	8	63	≤6	...	...	...	...	(N)
				15	257	<17					
2010−231	...	0.9	2	4.1	82	<4	<4	...	...	∼3	(N)
				15	212	<15	<15				
2020−211	...	2.1	2	8	106	∼25	∼16	117	86	0.7	(N)
				8	196	<10	<10				
2034−198	...	0.8	3	2.2	97	≤2.1	...	...	...	...	...
				2.2	194	<2					
2050−188	PKS 2050−18	2.1	2	1.2	76	∼2.4	<1	63	2.6	1.2	...
				1.2	219	∼1.5	<1				
2052−192	...	0.8	2	4.1	69	≤3	...	...	...	...	...
				4.1	223	≤3					
2057−179	PKS 2057−17	2.2	2	1.3	33	∼2	≤4	169	10	2.6	(N)
				2.1	278	≤3	≤4				
2058−179	PKS 2058−17	3.5	4	1.2	21	≤1.4	...	...	...	...	(N)
				2.1	71	∼3.3					
2113−163	...	0.3	2	10	71	≤8	<8	66	15	1	...
				10	218	<8	<8				
2120−166	PKS 2120−16	6.0	4	2.2	39	≤2	∼13	63	10	2.7	(N)
				1.3	281	≤1.3	∼11				
2123−155	...	0.5	3	8	235	∼12	...	...	...	...	...
				15	243	∼(20)					
2125−153.1	...	0.4	3	8	48	<6	...	...	...	...	...
				8	261	≤8					
2125−153.2	OX−143	0.5	4	4.2	223	<3	...	...	...	...	...
				4.2	247	<3					
2127−157	PKS 2126−15	0.7	6	4.1	67	∼4	...	...	...	...	...
				8	216	<7					
2154−129	...	1.0	3	10	32	∼29	...	...	...	...	Cx, (N)
				10	105	∼28					
2154−117	PKS 2154−11	3.0	2	2.2	97	∼3	∼3	18	21	1.6	(N)
				4.1	198	∼10	∼5				
2248−071	...	0.4	3	15	30	∼28	...	...	...	...	...
				15	54	∼30					

TABLE I (*continued*)

(1)	(2)	(3)	(4)	(5)	(6)	(7)		(8)	(9)	(10)	(11)
					Observed data			Derived structure			
Source OTL	Other catalog No.	Flux 327 MHz	No. of occult-ations	β_e	PA of occln.	Component sizes A	B	PA A to B	Comp. Sepn.	Flux ratio A/B	Remarks
2310−033	...	0.5	2	8 4.2	5 257	≤7 ≤4	...	...	...	...	...
2321−012	...	0.4	2	10 30	62 205	≤10 ≤25	...	...	...	...	...
2333−002	OZ−056	0.6	2	15 15	70 211	≤20 ∼16	...	...	...	...	(N)

Cx = Complex; PD = possibly double; (N) = Additional notes in text.

nature or otherwise of the redshifts of QSO's that may be associated with clusters (e.g., Hazard *et al.* 1973), the BSO identified with OTL 0208+183 appears to be an excellent candidate for spectroscopic investigation.

0246+219. Grazing occultation. Position and structure of component B are less accurately determined. There is a 15.5-mag spiral galaxy, about 4′.8 east and 0′.5 north of the radio position, with it's major axis pointing approximately in the direction of the radio source.

0505+278. About 30% of the total flux appears to be in a second component or tail extending to ∼45 arcsec southeast in PA ∼120°. This component is poorly determined.

0532+281. As the two components are not individually resolved in PA 24°, the component positions are not determined unambiguously. The alternate, less likely pairing, would imply a component separation of ∼13 arcsec in PA ∼148°.

0706+261. The positions of the two components determined by Hazard *et al.* (1967) from two occulations at 430 MHz are considerably displaced in declination from the positions obtained from the four occultations observed at Ooty, as shown in Fig. 1. It may be noted, however, that the position of the radio centroid measured recently by Ghigo and Owen (1973) at 365 MHz, with the Texas Broadband Synthesis Interferometer, is in excellent agreement with our occulation results. The optical object identified with the radio source is extremely faint (>20 mag) and just above the print limit of the E-print. There is a 15.5-mag E-galaxy about 35 arcsec east and 64 arcsec north, and a 17.5-mag BSO about two arcsec west and 18 arcsec north of the radio centroid.

0719+255. The emersion record (PA 290°) is affected by ionospheric scintillation. The source structure is elongated in PA 158°±15°. Most of the flux is probably in two roughly equal components separated by ∼40 arcsec. The brightness profile along PA 81° indicates that ∼25% of the total flux could be in an extended component upto ∼60 arcsec in extent towards increasing right ascension.

0817+212. The radio source lies close to the pair of galaxies NGC 2562 and 2563. The closer and brighter of the two—NGC 2563 (13.5-mag, SO)–is about 4′.2 west and 3′.6 south of the radio position.

0904+174. The emersion record (PA 285°) is affected by interference.

0907+185. In immersion (PA 100°) there appears to be a second component of about 0.8 f.u. It is probably spurious, being caused by a receiver instability. If real, it has an angular size of ∼8 arcsec and lies ∼34 arcsec west and ∼18 arcsec south of the definite component listed in Tables I and II.

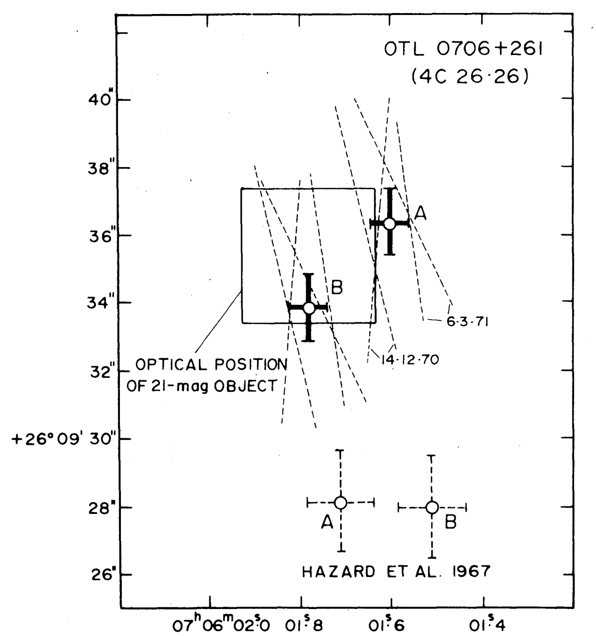

FIG. 1. The occultation positions of the components of 0706+261. Moon's limbs at the times of four occultations are shown be dotted lines.

TABLE II. Radio and optical positions and notes on the optical fields.

(1)	(2)		(3)		(4)	(5)	(6)		(7)	(8)
	Position (1950.0)									
	Radio				Optical		Radio-Opt.			
Source OTL	Right ascension		Declination		RA	Dec.	RA	Dec.	m_{pg}	Notes on optical objects
0023+058	$00^h23^m15^s.49$	$\pm0^s.07$	$+05°53'05''.8$	$\pm1''.5$	$(15^s.71$	$53'05''.0)$	$-3''$	$+1''$	21	Only in blue[b]
0134+142	01 34 00.16	0.1	+14 14 03.4	1.5	00.95	13 59.7	−12	+4	19	Red gal?
0141+157	01 41 07.14	0.1	+15 44 21.0	1.5	···	···	−42	+38	20	Stellar
0210+188	02 10 38.57	a	+18 48 54.5	a	38.92	49 14.8	−5	−20	19.5	Only in red, in cluster Zw 0210.1+1857; (N)
0210+190	02 10 47.63	0.07	+19 00 20.6	1	(48.15	00 34.6)	−7	−14	20	BSO? in cluster Zw 0210.1+1857; (N)
0246+219	A 02 46 18.76 B 02 46 19.03	0.1 0.15	+21 55 44.6 +21 55 52.7	1 3	17.30 ···	55 54.0 ···	+20 +24	−9 −1	16.5 ···	Red stellar, (N)
0246+217	02 46 36.48	a	+21 42 07.7	a	···	···	+23	−3	13.5	Stellar
0346+253	03 46 09.77	a	+25 22 33.5	a	08.29	22 27.7	+20	+6	16	Stellar
0505+278	A 05 05 04.61	0.15	+27 49 44.8	2	06.04	50 00.4	−19	−15	16	Stellar; $b^{II}=-7.4°$
0513+279	05 13 44.26	0.05	+27 55 39.5	0.7	(43.80	55 49.0)	+6	−10	20	Only in red; $b^{II}=-5.8°$
0532+281	(C)05 32 46.91	0.15	+28 09 31.1	1	···	···	···	···	···	Crowded field; $b^{II}=-2.2°$
0547+279	05 47 37.20	a	+27 55 41.0	a	···	···	···	···	···	Crowded field; $b^{II}=+0.5°$
0608+275	06 08 59.30	0.1	+27 31 33.1	1.5	(58.37	31 24.7)	+12	+8	18.5	Red stellar; $b^{II}=+4.4°$
0609+276	A 06 09 47.57 B 06 09 47.90	0.07 0.04	+27 37 45.1 +27 37 34.3	1 0.5	47.87 ···	37 46.9 ···	−4 0	−2 −13	16.5 ···	Red stellar; $b^{II}=+4.6°$
0618+272	06 18 16.89	0.07	+27 16 25.3	2	(16.44	16 19.1)	+6	+6	20	Crowded field; $b^{II}=+6.0°$
0619+270	06 19 50.87	0.1	+27 00 33.5	1.5	(50.16	00 30.8)	+9	+3	19.5	Stellar; $b^{II}=+6.2°$
0620+270	A 06 20 06.22 B 06 20 06.50	0.1 0.15	+27 03 57.0 +27 04 24.8	1.5 2	(06.09 ···	04 14.3) ···	+2 +5	−17 +11	20 ···	Gal; $b^{II}=+6.3°$[b]
0638+273	06 38 43.93	0.05	+27 18 09.6	0.7	43.61	18 17.4	+4	−8	18.5	Stellar
0706+261	A 07 06 01.60 B 07 06 01.78	0.05 0.04	+26 09 36.3 +26 09 33.8	1 1	(01.78 ···	09 35.5) ···	−2 0	+1 −2	21 ···	Only in red, (N)[b]
0719+255	(C)07 19 44.44	0.2	+25 34 14.0	3	45.36	34 22.3	−12	−8	16	E gal.[b] Merkelijn *et al.* (1968)
0725+244	07 25 29.13	a	+24 25 24.5	a	29.08	25 22.5	+1	+2	16	E gal.[b] Merkelijn *et al.* (1968)
0725+248	07 25 58.39	0.1	+24 52 40.9	1	02.50	52 17.4	−56	+24	16.5	Stellar
0817+212	A 08 17 58.55 B 08 17 59.24	0.07 0.15	+21 17 10.7 +21 17 05.6	1 2	(57.81 ···	16 55.9) ···	+10 +20	+15 +10	20 ···	BSO? (N)
0818+214	08 18 12.71	0.1	+21 26 22.5	1.5	(14.33	26 04.0)	−23	+19	20	Only in red
0818+217	A 08 18 43.30 B 08 18 44.90	a a	+21 44 04.3 +21 44 06.6	a a	44.10 ···	44 30.9 ···	−11 +11	−27 −24	14 ···	Stellar
0823+207	08 23 57.12	0.07	+20 46 44.4	1	57.58	46 47.0	−6	−3	19.5	N gal?
0854+191	08 54 41.39	0.07	+19 10 11.4	1	···	···	+40	0	19	Only in red
0856+178	08 56 46.31	0.1	+17 53 30.7	1.5	45.75	53 26.4	+9	+4	18	Red gal, in cluster Zw 0909.7+1814
0904+174	09 04 08.54	a	+17 27 35.3	a	···	···	−24	+28	20	Only in red
0907+185	09 07 06.48	0.07	+18 34 15.3	1	···	···	+16	+20	20	Very faint; three objects close together?

TABLE II (*continued*)

(1)	(2)		(3)		(4)	(5)	(6)		(7)	(8)
	Position (1950.0)									
	Radio				Optical		Radio-Opt.			
Source OTL	Right ascension		Declination		RA	Dec.	RA	Dec.	m_{pg}	Notes on optical objects
0909+165	(C)09ʰ09ᵐ17ˢ.08	a	+16°30′52″.6	a	15ˢ.46	30′55″.5	+23″	− 3″	18	Red gal; (N)
0937+144	09 37 48.89	±0ˢ.07	+14 29 57.7	±1″	···	···	−38	−56	17.5	Red stellar
0952+128	09 52 32.03	a	+12 48 53.8	a	···	···	+40	+20	18.5	BSO, (N)
0954+126	09 54 27.31	0.15	+12 36 30.0	1.5	···	···	− 7	−25	12.5	Stellar
0954+125	09 54 35.16	0.15	+12 33 42.6	1	···	···	−34	+10	19	gal.
1022+093	10 22 20.06	0.1	+09 21 17.0	2	18.52	21 09.9	+23	+ 7	12.5	Stellar
1037+067	10 37 39.20	0.07	+06 43 27.5	1	···	···	+40	+40	20	gal?
1038+064	10 38 40.83	0.15	+06 25 57.4	2	40.86	25 59.3	0	− 2	17	QSO, (N)[b] Wills and Bolton (1969)
1105+037	11 05 34.51	a	+03 43 40.4	a	···	···	−35	+35	20	Only in red, (N)
1123+012	11 23 20.58	0.07	+01 16 07.2	1	(20.63	16 06.9)	− 1	0	20	gal, in cluster Zw 1123.6+0118, (N)[b]
1155−029	11 55 16.51	0.1	−02 55 39.8	1	(16.42	55 40.4)	+ 1	+ 1	20	Only in red[b]
1239−086	12 39 56.73	a	−08 41 08.7	a	···	···	−40	0	20	BSO
1241−089	12 41 58.00	0.07	−08 59 00.8	2	56.89	59 33.5	+16	+33	20	Only in red
1253−109	12 53 40.73	0.04	−10 54 11.0	0.7	···	···	−46	−32	20	Only in red
1316−128	13 16 02.88	a	−12 51 31.2	a	···	···	−18	+22	16.5	Red stellar
1417−192	A 14 17 02.37	0.05	−19 15 06.3	0.5	01.33 02.36 02.66	15 13.5 14 53.1 14 41.1	+15 0 − 4	+ 7 −13 −25	19.5 20 17.5	db gal? gal. N gal, (N)
1431−202	14 31 22.56	a	−20 16 00.0	a	21.39	16 06.4	+16	+ 6	18	Red stellar
1547−254	15 47 24.44	0.07	−25 28 07.6	1	(22.71	27 52.9)	+23	−15	20	Brighter in red
1628−268	A 16 28 33.25	0.05	−26 50 15.8	0.5	···	···	···	···	···	Crowded field, (N)
1650−283	16 50 45.60	0.1	−28 18 23.5	2.5	···	···	···	···	···	Crowded field, $b^{II}=+9.6°$
1653−281	16 53 38.92	0.04	−28 08 54.6	0.5	···	···	···	···	···	Crowded field, $b^{II}=+9.2°$
1657−281	(C)16 57 54.7	0.3	−28 11 13.5	4	···	···	···	···	···	Crowded field, $b^{II}=+8.5°$
1709−281	A 17 09 48.35 B 17 09 48.98	0.04 0.05	−28 05 59.3 −28 06 11.5	0.5 0.7	··· ···	··· ···	··· ···	··· ···	··· ···	Crowded field, $b^{II}=+6.4°$
1711−285	17 11 18.22	0.07	−28 33 04.2	1	···	···	···	···	···	Crowded field, $b^{II}=+5.9°$
1800−278	A 18 00 07.44 B 18 00 08.61	0.1 0.1	−27 48 04.7 −27 48 44.9	1.5 2	··· ···	··· ···	··· ···	··· ···	··· ···	Crowded field, $b^{II}=-2.8°$
1818−269	18 18 42.59	0.2	−26 57 24.6	3	···	···	···	···	···	Crowded field, $b^{II}=-6.0°$
1827−279	18 27 12.78	a	−27 54 56.8	a	···	···	···	···	···	Crowded field, $b^{II}=-8.1°$
2010−231	(C)20 10 17.10	0.15	−23 06 08.0	3	17.84	06 08.8	−10	+ 1	16	Red, Stellar? (N)[b]
2020−211	A 20 19 59.40 B 20 20 04.87	0.2 0.15	−21 06 00.0 −21 06 38.7	3 2	04.65 ···	06 38.1 ···	−73 + 3	+38 − 1	15.5 ···	D gal; Brightest in cluster, (N)[b]
2034−198	20 34 18.61	0.05	−19 52 32.6	0.7	18.62	52 33.2	0 + 2	+ 1 + 8	18 19	Red gal.[b] Red gal.
2050−188	A 20 50 28.23 B 20 50 28.40	0.07 0.07	−18 50 19.6 −18 50 18.5	1 1	29.37 ···	50 23.5 ···	−16 −14	+ 4 + 5	12.5 ···	Stellar with a jet in PA ∼150°

TABLE II (*continued*)

(1) Source OTL	(2) Position (1950.0) Radio: Right ascension		(3) Radio: Declination		(4) Optical: RA	(5) Optical: Dec.	(6) Radio-Opt.: RA	Radio-Opt.: Dec.	(7) m_{pg}	(8) Notes on optical objects
2052−192	20ʰ52ᵐ57ˢ.78	a	−19°17′14″.9	a	57ˢ.96	17′16″.3	− 3″	+ 1″	20	BSO, only in blue[b]
2057−179	(C)20 57 26.17	±0ˢ.07	−17 57 33.8	±1″.5	25.52	57 30.4	...	...	17	Stellar, (N)
	A 20 57 26.13	0.07	−17 57 30.9	1	...	...	+ 9	− 1	...	
	B 20 57 26.26	0.1	−17 57 40.8	2	...	...	+11	−10	...	
2058−179	20 58 54.31	0.04	−17 59 48.8	0.5	(54.18	59 49.1)	+ 2	0	19.5	BSO? (N)[b]
					53.72	00 05.7	+ 8	+17	18	BSO
2113−163	(C)21 13 34.84	0.1	−16 20 57.2	1.5	35.94	21 04.9	−16	+ 8	18	Stellar
2120−166	A 21 20 15.12	0.04	−16 40 49.4	0.5	(15.39	40 35.9)	− 4	−14	20	Stellar, (N)
	B 21 20 15.75	0.07	−16 40 44.9	1	...	...	+ 5	− 9	...	
2123−155	21 23 37.99	a	−15 33 58.6	a	(37.96	34 02.8)	0	+ 4	20	BSO? only in blue[b]
2125−153.1	21 25 03.73	0.07	−15 18 11.3	2	03.00	18 24.1	+11	+13	14	Stellar
2125−153.2	21 25 37.04	a	−15 18 04.4	a	36.74	18 00.3	+ 4	− 4	19	Blue gal? (N)[b]
2127−157	21 27 02.27	0.07	−15 42 12.8	1	...	...	+13	+39	17	Stellar
2154−129	(C)21 54 00.25	0.1	−12 54 07.5	1	00.41	54 06.2	− 2	− 1	16.5	D gal, brightest in cluster[b]
2154−117	(C)21 54 03.24	0.07	−11 42 09.3	1.5	02.89	41 20.3	+ 5	−49	19.5	gal.
	A 21 54 03.09	0.07	−11 42 15.9	1.5	...	...	...	...	...	
	B 21 54 03.54	0.1	−11 41 55.8	1.5	...	...	...	...	...	
2248−071	22 48 35.20	a	−07 11 13.6	a	(36.68	10 45.7)	−22	−28	19	BSO, only in blue
2310−033	23 10 59.82	0.1	−03 19 13.4	1.5	(00.79	19 15.4)	−15	+ 2	18	BSO
2321−012	23 21 29.7	0.3	−01 15 11	4	...	...	0	+35	20	gal, only in red
2333−002	23 33 49.62	0.15	−00 14 08	4	50.21	13 51.4	− 9	−17	17	BSO

[a] Position errors:
0210+188: ±1.5″ in PA 62° and ±8″ in PA 152°
0246+217: 1.5″ in PA 78° and 5″ in PA 168°
0346+253: 1″ in PA 84° and 12″ in PA 174°
0547+279: 1.5″ in PA 85° and 5″ in PA 175°
0725+244: 0.7″ in PA 127° and 3″ in PA 37°
0818+217A: 2″ in PA 114° and 7″ in PA 24°
0818+217B: 1″ in PA 125° and 2.5″ in PA 35°
0904+174: 1.5″ in PA 96° and 15″ in PA 06°
0909+165: 1″ in PA 142° and 3″ in PA 52°
0952+128: 1.5″ in PA 127° and 15″ in PA 37°
1105+037: 1″ in PA 130° and 4″ in PA 40°
1239−086: 0.5″ in PA 136° and 2″ in PA 46°
1316−128: 1.5″ in PA 130° and 10″ in PA 40°
1431−202: 1.5″ in PA 105° and 10″ in PA 15°
1827−279: 2″ in PA 70° and 8″ in PA 160°
2052−192: 0.7″ in PA 69° and 3″ in PA 159°
2123−155: 1.5″ in PA 59° and 7″ in PA 149°
2125−153.2: 1″ in PA 44° and 4″ in PA 134°
2248−071: 2″ in PA 45° and 5″ in PA 135°.

[b] Positive or likely identification.
(N) Additional notes in text.

0909+165. The presence of ionospheric scintillation during emersion, limits the resolution in PA 294°. In PA 142°, the source is clearly double, and the stronger component appears to have an extension towards the other component (Fig. 2). The optical identification with an 18.5-mag E-galaxy (marked in Fig. 2) suggested by Bolton and Ekers (1966a) is not supported by the present observations. A 15-mag E-galaxy lies 2′.7 west and 1′.85 south of the radio centroid and has its major axis pointing in the direction of the radio source.

0952+128. The occultation is affected by ionospheric scintillation. As the two points of intersection of the Moon's limbs at the times of occultation lie within about 40 arcsec in declination, there is some doubt about the choice of the correct position. The alternate

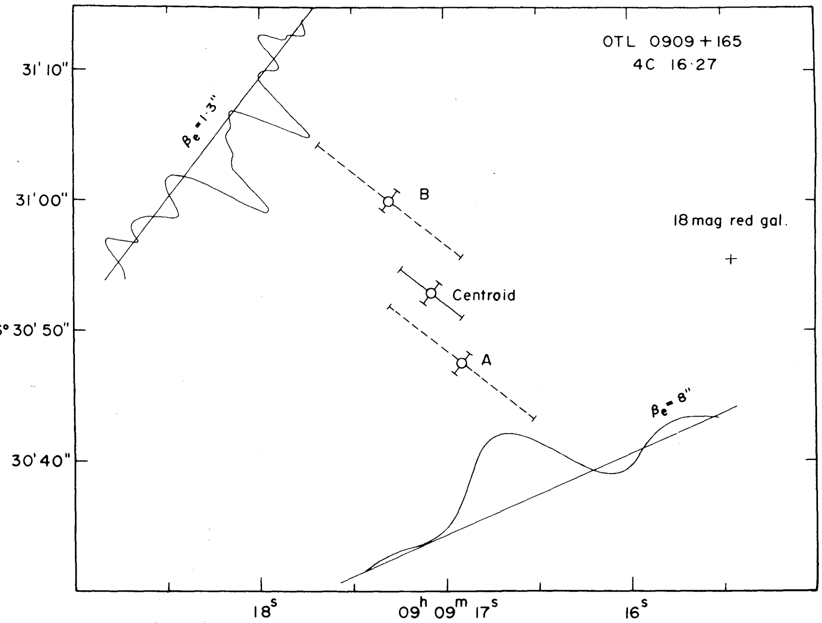

FIG. 2. Brightness profiles across 0909+165 plotted along the appropriate position angles of occultations.

less likely position is at $09^h52^m34\overset{s}{.}05$ and $+12°49'33\overset{''}{.}2$, with an error of $\pm1\overset{''}{.}5$ in PA 127° and ±15 arcsec in PA 37°.

0954+125. A possible second component ~20 arcsec west in PA 253° with ≤30% of the total flux.

1037+067 and 1038+064. Occultation observations show that the source 4C 06.41 in the 4C catalog (Gower *et al.* 1967) is a blend of these two sources whose right ascensions lie one lobeshift (~$7\overset{'}{.}5$) earlier and later respectively, than the 4C value. The observations of 4C 06.41 by Clarke *et al.* (1969) at 408 MHz, and Wills and Bolton (1969) at 2.7 GHz, refer only to 1038+064. Three of the four occultations of 1037+067 are affected by ionospheric scintillation. Both the occultations of 1038+064 show the presence of interplanetary scintillations, implying angular structure <1 arcsec. The QSO identified with 1038+064 (Wills and Bolton 1969) has $V=16.81$ and redshift $z=1.270$ (Lynds and Wills 1972). There are several galaxies of 15–16 mag within five to ten arcmin of the quasar.

The flux measurements of Wills and Bolton (1969) for 1038+064 at 2.7 GHz and of T. K. Menon (private communication) for both the sources at 1.4 and 2.7 GHz, show that between 327 MHz and 2.7 GHz, 1037+067 has a spectral index (defined by $S\alpha\nu^{\alpha}$) of $\alpha\sim-0.75$ and 1038+064 has a flat spectrum with $\alpha\sim0.0\pm0.1$.

1105+037. There is a 14.5-mag *E*-galaxy about $3\overset{'}{.}7$ east and $2\overset{'}{.}4$ north of the radio position.

1123+012. Possibly double with a component separation of ~3 arcsec in PA ~150° or ~$2\overset{''}{.}5$ in PA ~30°. The source is likely to be associated with the cluster Zw 1123.6+0118 which has been classified as Extremely Distant, medium compact, and has a 'diameter' of ~9 arcmin (Zwicky *et al.* 1961).

1417−192. Brightness profiles along the five PA's and a schematic source model are shown in Fig. 3. About 55% of the total flux is in the 'head' component, A, which has an angular size of ~$7\overset{''}{.}5\times4$ arcsec, with its major axis in PA 145°±10°. The remaining flux is

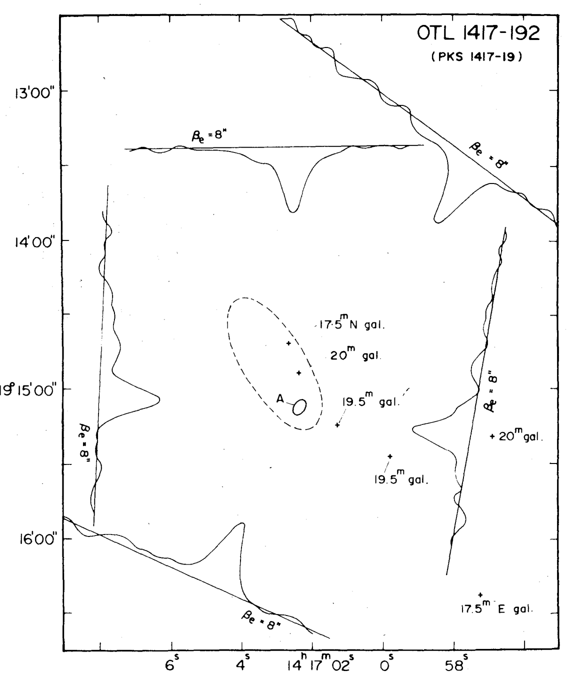

FIG. 3. Strip brightness distributions along five position angles and a schematic model for 1417−192.

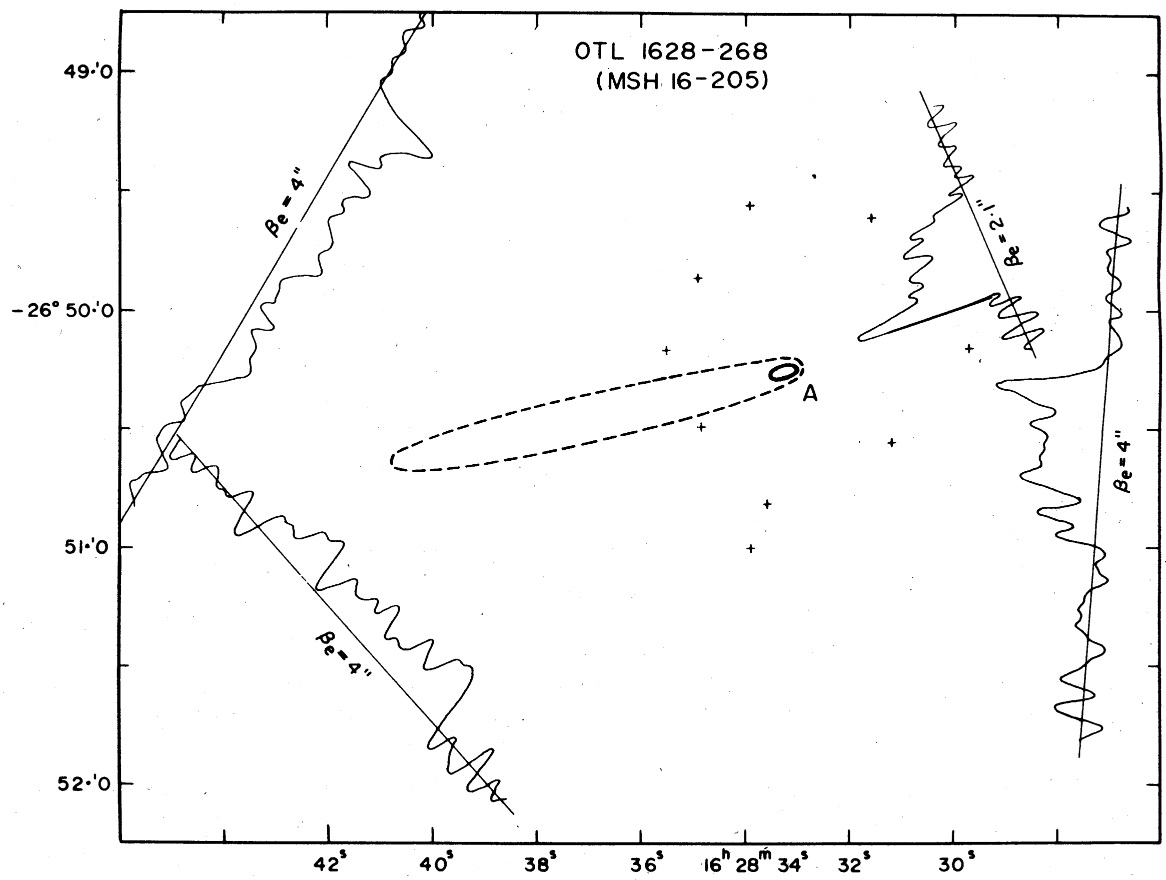

FIG. 4. Brightness profiles and a schematic model for 1628−268. Optical positions of objects are shown by crosses (+).

in a 'tail' that extends to nearly 60 arcsec northeast along PA 30°±10°. The width of the tail is <25 arcsec.

The brightness distribution appears to be similar to that exhibited by 'head tail' galaxies in some rich clusters (Hill and Longair 1971, Miley 1973). There are several galaxies in the region of the radio source, and their positions and magnitudes are shown in Fig. 3. Bolton and Ekers (1966b) have identified the source with the 17.5-mag N-galaxy which has a redshift of $z=0.1192$ (Burbidge 1967). No definite identification with any single galaxy can however be established, as is clear from Fig. 3. It is very interesting to note that nearly all the galaxies in the region lie approximately along a straight line defined by the axis of the 'tail' component and further, the major axis of the 17.5-mag E-galaxy, which is the brightest in the chain, also lies approximately in the same position angle. These suggest a physical association of the radio source with the chain of galaxies. Assuming the source to be at the distance indicated by the redshift of the N-galaxy, the linear extent of the 'tail' of 1417−192 (~100 kpc for $H=100$ km sec^{-1} Mpc^{-1}, and $q_o=\frac{1}{2}$) is comparable to that of other known 'head–tail' galaxies, but the luminosity (~7×10^{24} W Hz^{-1} Ster^{-1} at 327 MHz) is about an order of magnitude higher.

1628−268. This source also has a 'head–tail' structure, illustrated schematically in Fig. 4. About 29±2% of the total flux is in the head-component A which has an angular extent of ~7×3 arcsec, and is elongated in PA 95±10°. The remaining flux is in the tail that extends eastwards from the head for ~105 arcsec in PA 103±3°. The angular width of the tail is <15 arcsec. The optical field in the region of the radio source ($b^{II}=+14.^{\circ}4$) appears crowded. Objects close to the source (Fig. 4) are either red stellar or are too faint to be classified. There does not appear to be a cluster in the region.

1657−281. Two of the occultations are of poorer quality.

1709−281. Three of the occultations are affected by ionospheric scintillation. The two components appear slightly elongated along the line of separation and about 15%–20% of the total flux is in weak tails extending about 4 or 5 arcsec inwards from the two components.

1800−278. A bridge connecting the two components accounts for about 15% of the total flux. Slee and Higgins (1973) have given an upper limit of 10 f.u. for the flux at 80 MHz, as they did not detect the source

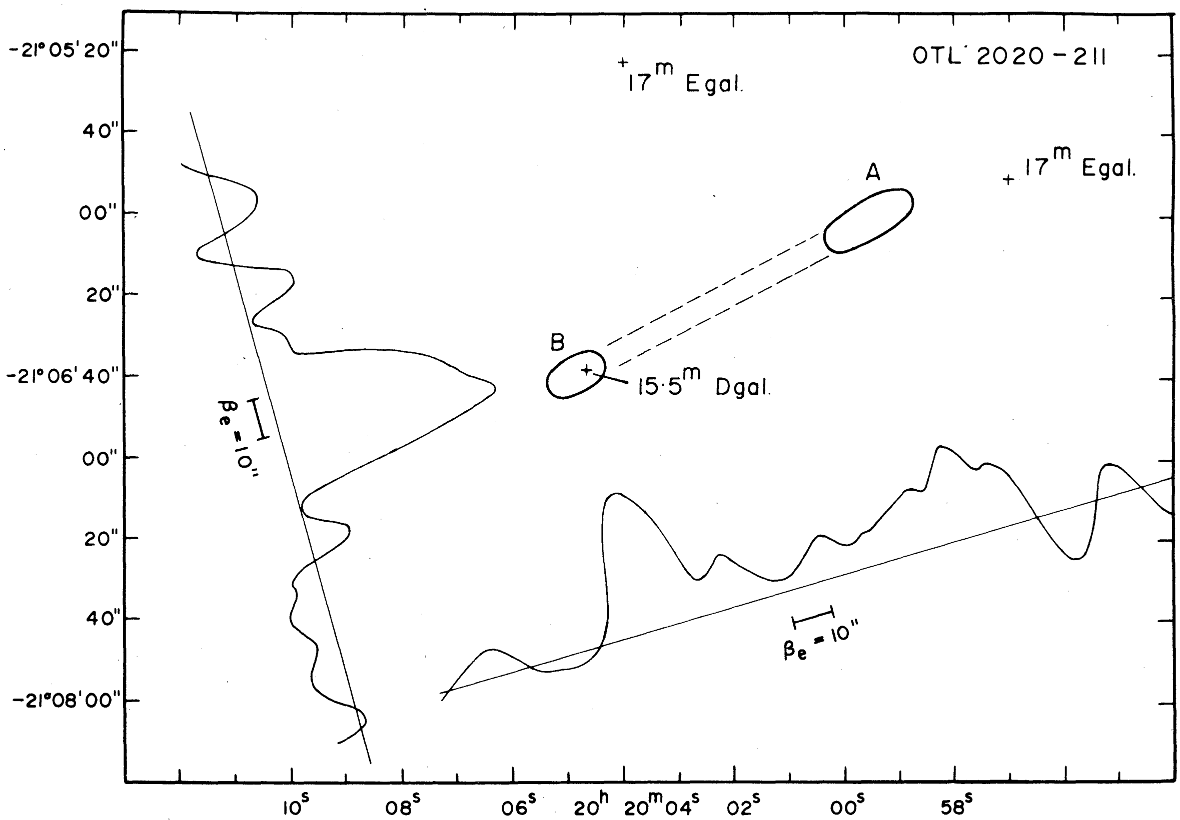

FIG. 5. Strip distributions and source model for 2020−211.

with the Culgoora radioheliograph. The region of the sky around the source covered by the radioheliograph beams would not, however, have included the source as the true declination lies about 12 arcmin North of the position given in the MSH catalog (Mills *et al.* 1960).

1827−279. Ionospheric scintillation during emersion (PA 257°).

2010−231. In immersion (PA 82°) the source is resolved into two components (flux ratio ~3), the weaker lying ~13 arcsec east of the stronger component. The emersion (PA 212°) is affected by ionospheric scintillation and it is not possible to resolve the components. The 16-mag red object appears slightly nonstellar in the O-print. It is, therefore, suggested as a likely identification.

2020−211. A schematic model for the brightness distribution is shown in Fig. 5. The stronger and more compact component, B, coincides with a 15.5-mag D-galaxy which appears to be the brightest in a cluster. About one-third of the total flux is in the 'bridge' connecting the two components. Morphologically, the source structure is similar to that of OTL 0911+174 (4C 17.48), which also has two resolved components connected by a bridge (Kapahi *et al.* 1973b) with the stronger and more compact component coinciding with an 18-mag BSO.

2057−179. Hazard (1972) has reported one occultation of the source at 410 MHz, and finds an angular size of ~7 arsec in PA 120°. The possible nearby source of about 1 f.u., ~100 arcsec away from 2057−179, noted by Hazard on his occultation record was not observed at Ooty and is, therefore, likely to be spurious. The 18.5-mag galaxy suggested as a probable identification by Hazard, lies 3 arcsec west and 25 arcsec south of the radio centroid.

2058−179. The source is elongated along PA 128±10° and has an angular size of ~4×<1.4 arcsec. Interplanetary scintillation observations at 327 MHz (Bhandari *et al.* 1974) indicate that ~30% of the flux in the source is contained in a component of angular size <0.15 arcsec .The BSO? identified with the source has a slightly nonstellar appearance in blue. It is just above the print limit in red. The optical identification with an 18-mag BSO (whose optical position is given in Table II) proposed by Bolton *et al.* (1971), is not supported by the present observations.

2120−166. The weaker component is possibly like a tail of length about 13 arcsec and elongated along PA ~63°. In the perpendicular direction, the 'tail'

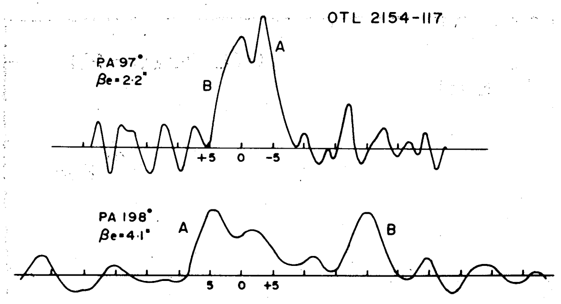

FIG. 6. Strip brightness profiles across 2154−117.

has an angular size <10 arcsec. The orientation, separation, and flux ratio of the components in the source model derived by Critchley *et al.* (1972) at 408 MHz, from interferometric observations with a 24-km base line, are in broad agreement with the occultation results. The component sizes of 3 arcsec derived by them are, however, not surpported by the occultation results.

There is a faint object (>20 mag) barely visible only in the blue print of the Sky Survey, about 20 arcsec Northeast of component 'A' along PA ~60°.

2125−153.2. The optical object identified with the source is about 1 mag fainter in red and appears nonstellar.

2154−129. Two of the three occultations observed are of poorer quality. The simplest interpretation of the brightness distributions is a double with component separation of 27±5 arcsec in PA 160±15°, the more westerly component being 1.4±0.2 times stronger. The components are resolved and have angular sizes of 12±3 arcsec.

2154−117. The stronger component, A, appears to be extended inwards towards the other component (Fig. 6).

2333−002. Occultation affected by ionospheric scintillation.

ACKNOWLEDGMENTS

We are grateful to Professor G. Swarup for his interest and valuable comments. We thank C. R. Subrahmanya for help with optical identifications and Professor M. K. Vainu Bappu for kindly providing the facilities for identification work at the Indian Institute of Astrophysics, Kodaikanal.

REFERENCES

Bhandari, S. M., Ananthakrishnan, S., and Rao, A. P. (1974). Aust. J. Phys. To be published.
Bolton, J. G., and Ekers, J. (1966a). Aust. J. Phys. **19**, 471.
Bolton, J. G., and Ekers, J. (1966b). Aust. J. Phys. **19**, 559.
Bolton, J. G., Wall, J. V., and Shimmins, A. J. (1971). Aust. J. Phys. **24**, 889.
Burbidge, E. M. (1967). Astrophys. J. **149**, L51.
Clarke, T. W., Frater, R. H., Large, M. I., Munro, R. E. B., and Mardoch, H. S. (1969). Aust. J. Phys. Astrophys. Suppl., No. 10.
Critchley, J., Palmer, H. P., and Rowson, B., (1972). Mon. Not. R. Astron. Soc. **160**, 271.
Ghigo, F. D., and Owen, F. N. (1973). Astron. J. **78**, 848.
Gower, J. F. R., Scott, P. F., and Wills, D. (1967). Mem. R. Astron. Soc. **71**, 49.
Hazard, C., Gulkis, S., and Bray, A. D. (1967). Astrophys. J. **148**, 669.
Hazard, C., (1972). Astrophys. Lett. **11**, 139.
Hazard, C., Jauncey, D. L., Sargent, W. L. W., Baldwin, J. A., and Wampler, E. J. (1973). Nature **246**, 205.
Hill, J. M., and Longair, M. S. (1971). Mon. Not. R. Astron. Soc. **154**, 125.
Joshi, M. N., Kapahi, V. K., Gopal-Krishna, Sarma, N. V. G., and Swarup, G. (1973). Astron. J. **78**, 1023.
Kapahi, V. K. (1971). Nature Phys. Sci. **234**, 49.
Kapahi, V. K., Joshi, M. N., and Gopal-Krishna (1972). Astrophys. Lett. **11**, 155.
Kapahi, V. K., Joshi, M. N., and Kandaswamy, J. (1973a). Astrophys. Lett. **14**, 31.
Kapahi, V. K., Joshi, M. N., Subrahmanya, C. R., and Gopal-Krishna (1973b). Astron. J. **78**, 673.
Lynds, R., and Wills, D. (1972). Astrophys. J. **172**, 531.
Merkelijn, J. K., Shimmins, A. J., and Bolton, J. G. (1968). Aust. J. Phys. **21**, 523.
Miley, G. K. (1973). Astron. Astrophys. **26**, 413.
Mills, B. Y., Slee, O. B., and Hill, E. R. (1960). Aust. J. Phys. **13**, 676.
Slee, O. B., and Higgins, C. S. (1973). Aust. J. Phys. Astrophys. Suppl., No. 27.
Swarup, G., Kapahi, V. K., Sarma, N. V. G., Gopal-Krishna, Joshi, M. N., and Rao, A. P. (1971). Astrophys. Lett. **9**, 53.
Wills, D., and Bolton, J. G. (1969). Aust. J. Phys. **22**, 775.
Zwicky, F., Herzog, E., and Wild, P. (1961). Catalogue of Galaxies and of Clusters of Galaxies, Vol. I (Calif. Inst. Tech.).
Zwicky, F., Karpowicz, M., and Kowal, C. T. (1965). Catalogue of Galaxies and Clusters of Galaxies, Vol. V (Calif. Inst. Tech.).

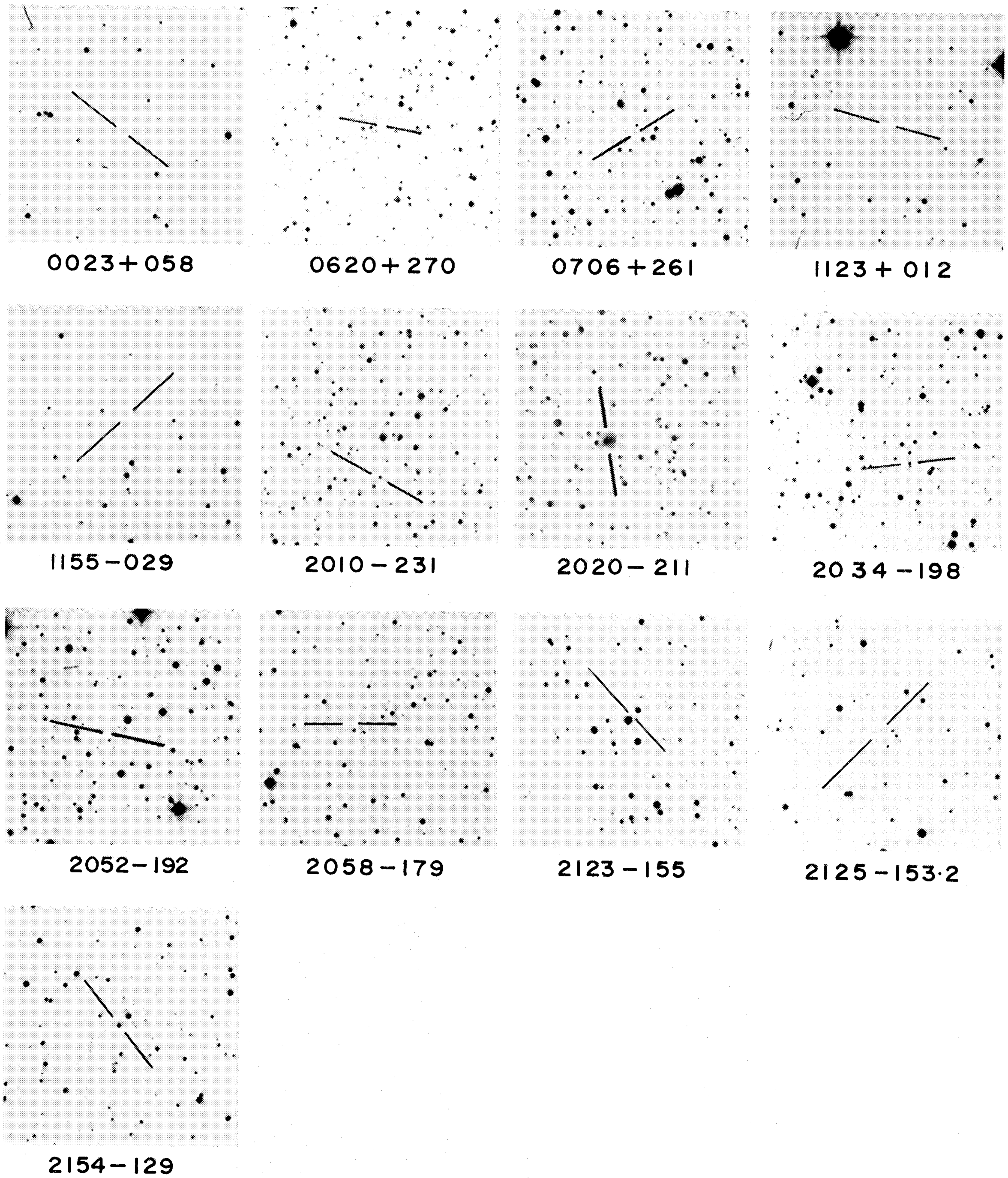

PLATE I (Kapahi, Joshi, and Sarma, p. 515). Finding charts for 13 radio sources. North is at the top and east at the left. The field shown covers about nine arcmin on the side.